MICROBIOLOGY

Lack of nutritional immunity in diabetic skin infections promotes *Staphylococcus aureus* virulence

Lance R. Thurlow, Amelia C. Stephens, Kelly E. Hurley, Anthony R. Richardson*

Elevated blood/tissue glucose is a hallmark feature of advanced diabetes, and people with diabetes are prone to more frequent and invasive infections with *Staphylococcus aureus*. Phagocytes must markedly increase glucose consumption during infection to generate and oxidative burst and kill invading bacteria. Similarly, glucose is essential for *S. aureus* survival in an infection and competition with the host, for this limited resource is reminiscent of nutritional immunity. Here, we show that infiltrating phagocytes do not express their high-efficiency glucose transporters in modeled diabetic infections, resulting in a diminished respiratory burst and increased glucose availability for *S. aureus*. We show that excess glucose in these hyperglycemic abscesses significantly enhances *S. aureus* virulence potential, resulting in worse infection outcomes. Last, we show that two glucose transporters recently acquired by *S. aureus* are essential for excess virulence factor production and the concomitant increase in disease severity in hyperglycemic infections.

INTRODUCTION

The incidence of diabetes is rapidly increasing, with some estimates predicting more than 590 million afflicted people by 2035 (*1*). Several complications are associated with diabetes including increased risk of infection (*2*). One of the most common infections in individuals with diabetes are skin and soft tissue infections (SSTIs) that often manifest as foot ulcers (*2*, *3*). SSTIs in people with diabetes are often polymicrobial; however, *Staphylococcus aureus* is the most commonly isolated pathogen from diabetic SSTIs (*4*, *5*). Moreover, *S. aureus* SSTIs more frequently result in invasive infections, including endocarditis, osteomyelitis, and sepsis in patients with diabetes (*3*, *4*). Numerous studies have revealed defects in both innate and adaptive immunity that are attributed to the diabetic state and contribute to the severity of infections. These include decreased reactive oxygen species (ROS) production by neutrophils and suppressed T cell function; however, the mechanisms for suppressed immunity are not known (*6*–*9*). While immune suppression in diabetic infections has been described numerous times, to our knowledge, there have been few studies that address how hyperglycemia in diabetic infections influences the virulence potential of bacterial pathogens.

To cause disease, *S. aureus* must produce several secreted virulence factors including, but not limited to, α-hemolysin (Hla), phenol-soluble modulins (PSMs), and various proteases. Most of these virulence factors are unique to *S. aureus* and not found in other staphylococcal species (*10*, *11*). In addition, for full virulence, *S. aureus* must metabolically adapt to immune radical laden and hypoxic environments within sites of inflammation. This trait too distinguishes *S. aureus* from most other species of staphylococci. One unifying feature of maximized virulence factor production and respiration-independent fermentation in *S. aureus* is that both require access to abundant carbohydrates, specifically glucose. Accordingly, *S. aureus* has evolved an expanded glycolytic capacity, highlighted by the acquisition of two additional glucose transporters: GlcA and GlcC (*12*). While these two phosphotransferase system (PTS)–dependent glucose transporters are found in the genomes of virtually every *S. aureus* clone, they are largely absent from coagulase-negative staphylococcal species (*12*).

Several bacterial species rely on quorum sensing to monitor cell density and regulate the expression of a spectrum of genes including virulence factors. In *S. aureus*, the accessory gene regulator (Agr) is the primary quorum sensing system responsible for inducing the transcription of several virulence factors (*13*–*15*). The Agr operon consists of four genes, an autoinducing peptide (AIP) encoded by *agrD*, the peptide transporter/processor *agrB*, the receptor histidine kinase *agrC*, and the response regulator *agrA*. During growth, AIP accumulates in the environment and is sensed by AgrC that subsequently autophosphorylates and passes its phosphoryl group to AgrA. Phosphorylated AgrA acts as a transcriptional activator that induces the transcription of many virulence factors including PSMs and the Agr operon itself as well as RNAIII, which is responsible for full expression of toxins (*16*, *17*). A recent study showed that the adenosine 5′-triphosphate (ATP)–binding domain of *S. aureus* AgrC has reduced affinity for ATP relative to other sensor kinases, requiring up to 10 times more intracellular ATP for full AgrC activity (*18*, *19*). This study further suggested that linkage between Agr activity and intracellular ATP levels affords *S. aureus* the ability to "sense" the energy status of the cell via the Agr system. Thus, toxin production in *S. aureus* is controlled by bacterial density and a positive energy status.

Here, we show that exacerbated disease severity in a murine model of diabetes can be attributed to two aspects of this metabolic state: innate immune dysfunction and hyperglycemia. We used a streptozotocin (STZ)–induced hyperglycemia to model particular aspects of diabetes. Namely, by specifically killing β cells of the pancreas, STZ induces insulin-dependent hyperglycemia within 48 to 72 hours following injection. Subsequent inoculation with *S. aureus* allowed for assessing the effects of hyperglycemia on virulence factor production and disease outcomes while avoiding the confounding effects of advanced age and obesity associated with other murine models of diabetes. Given the poor immune output of phagocytes from STZ-treated animals, *S. aureus* is able to reach much higher densities than in the abscesses from untreated euglycemic animals. In addition, we show that the lack of glucose consumption by phagocytes from STZ-treated mice partly explains the previous

Department of Microbiology and Molecular Genetics, University of Pittsburgh, Pittsburgh, PA 15219, USA.
*Corresponding author. Email: anthony.richardson@pitt.edu

observations of diminished respiratory burst. The lack of glucose consumption by these phagocytes coupled with total body hyperglycemia results in an infection environment that is replete with the excess glucose. We show that the excess glucose in infections of STZ-treated animals maximizes *S. aureus* virulence factor production in an Agr-dependent fashion. Furthermore, our results demonstrate that mutants defective in glycolysis are limited in virulence factor production and cannot cause severe lesions in hyperglycemic infections. Last, we show that the evolved expansion of glycolytic capacity in *S. aureus* is required for excessive invasiveness in hyperglycemic SSTIs. Specifically, we show that the recent acquisition of *glcA* and *glcC* by *S. aureus* is essential for full toxin production and virulence potential in hyperglycemic SSTIs.

RESULTS

Infiltrating phagocytes do not consume glucose or generate and oxidative burst in hyperglycemic infections

We used an STZ-induced diabetic mouse model to compare the severity and invasiveness of *S. aureus* SSTIs between hyperglycemic and euglycemic (untreated) mice. Mice were injected subcutaneously with 10^7 colony-forming units (CFUs) of *S. aureus* and were assessed 7 days after infection for weight loss, lesion size, bacterial burdens within the abscess, and dissemination to peripheral organs. Our results show that hyperglycemic STZ-treated mice develop more severe infections than their untreated counterparts in every measured metric. STZ-treated mice displayed increased lesion size, excessive weight loss, elevated bacterial burden in the infected abscess, and increased dissemination to peripheral organs (Fig. 1, A to E, and fig. S1, A to C). This is consistent with other diabetic SSTI models with *S. aureus*.

People with diabetes are known have innate immune defects that contribute to infection severity. The most common innate immune defect described in diabetic infections is the lack of an oxidative burst consisting of ROS and nitric oxide (NO·) generated by macrophages and neutrophils (*9*). When activated, innate immune cells undergo a substantial metabolic reprogramming reminiscent of Warburg metabolism where glycolysis is significantly increased with pyruvate being converted to lactate instead of being fluxed through the tricarboxylic acid (TCA) cycle (*20*). The rapid influx of glucose needed for oxidative burst necessitates the expression of high-affinity glucose transporters encoded by *SCL2A1* and *SCL2A3* commonly referred to glucose transporter-1 and -3 (GLUT-1/-3) (*21*). To determine the importance of host glucose utilization to *S. aureus* immunity, we deprived RAW 264.7 macrophages of glucose and expectedly found that the absence of glucose prevents macrophages from generating an oxidative burst and attenuates their ability to kill *S. aureus* in vitro (fig. S2, C and D). Immunohistochemistry (IHC) performed on infected tissues revealed that immune cells in both untreated and STZ-treated mice expressed inducible NO synthase (iNOS); however, similar to what has previously been described, we observed almost no evidence of oxidative burst in abscess tissues from STZ-treated animals by the absence of nitrotyrosine adducts that are only formed in the presence of high levels of ROS and NO (Fig. 1, F and G). Furthermore, we observed that iNOS-positive infiltrating cells at the infection site in untreated mice stained brightly for GLUT-1 and GLUT-3; however, we detected neither in infected tissue from STZ-treated animals even though infiltrating cells were present (Fig. 1H and fig. S1, A and B). We subsequently infected

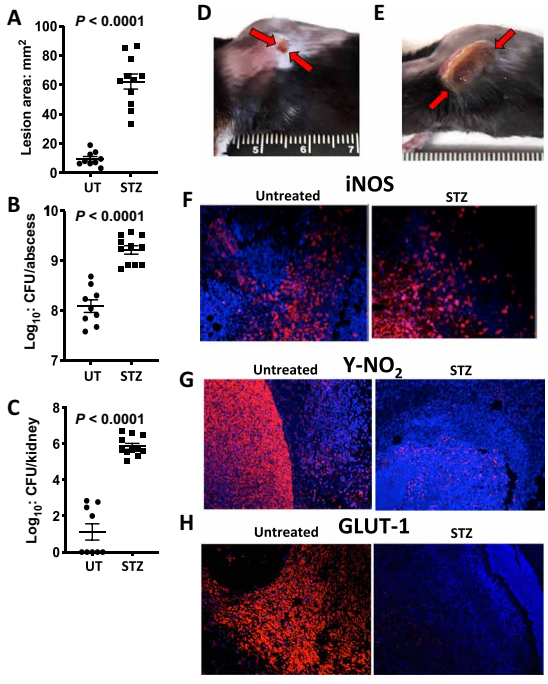

Fig. 1. Diminished oxidative burst in hyperglycemic abscesses correlates with worse infection outcomes. Untreated (UT) ($N = 9$ and $N = 11$) and STZ-treated ($N = 11$ and $N = 8$) mice were infected with 1×10^7 CFU of the USA300 methicillin-resistant *S. aureus* (MRSA) strain LAC. WT-infected STZ-treated mice have a larger dermonecrotic lesion (**A**), increased abscess burden (**B**), and increased dissemination to the kidney (**C**) compared with similarly infected untreated mice. Pictures of dermonecrotic lesions from an untreated mouse (red arrows) (**D**) and a STZ-treated mouse (**E**) show enhanced dermonecrosis in hyperglycemic infection. Immunohistochemistry (IHC) was performed on tissues from untreated and STZ-treated infections using antibodies against iNOS, nitrotyrosine (Y-NO_2), or GLUT-1 (red) and counterstained with 4′,6-diamidino-2-phenylindole (DAPI) (blue). (**F**) Tissues from both untreated and STZ-treated mice show iNOS staining. (**G**) However, while untreated mice exhibit robust Y-NO_2 staining, this adduct is largely absent in tissue from STZ-treated animals. (**H**) Similarly, tissues from untreated mice show robust GLUT-1 staining that is mostly absent in tissue from STZ-treated animals. Photo credit: Lance Thurlow, University of Pittsburgh.

LysM/Cre GLUT-1 knockout (KO) mice that do not express GLUT-1 on macrophages or neutrophils to confirm that maximum host glucose utilization is necessary for oxidative burst and control of *S. aureus* infections. Similar to what we observed in diabetic mice, IHC from GLUT-1 KO mice showed no GLUT-1 expression concomitant with the absence of nitrotyrosine adducts (fig. S3, A to D). In addition, GLUT-1 KO mice displayed increased bacterial burdens in the abscess and increased dissemination to peripheral organs, albeit to a lesser extent than in STZ-treated mice (fig. S3, E and F). Thus, with all other aspects of insulin signaling intact, the limited host glycolytic flux in GLUT-$1^{-/-}$ mice results in reduced ability to control *S. aureus* infections.

The Agr two-component system is essential for invasive hyperglycemic infections and requires glucose for activation

Our results show that STZ-treated mice develop more severe infections than their untreated counterparts in every measured metric. STZ-treated animals exhibit elevated blood glucose (≥300 mg/dl compared with ~100 mg/dl in untreated animals), which translates

into significantly elevated tissue glucose levels (>4-fold) at the site of infection (Fig. 2A). Furthermore, others and we observed that glucose promotes Agr-mediated toxin production by *S. aureus* (*22*, *23*). The Agr regulated RNAIII is responsible for maximal toxin and protease expression. The presence of glucose is known to enhance Agr activity when grown in buffered conditions (*23*). We cultivated *S. aureus* in chemically defined media (CDM) supplemented with glucose (PNG) or casamino acids (PNCAA) to determine whether glucose preferentially activated RNAIII transcription using an RNAIII yellow fluorescent protein (YFP) fusion. Our results confirm a significant increase in RNAIII-driven YFP in strains grown in PNG compared with PNCAA (Fig. 2, B and C).

In *S. aureus*, the Agr two-component system is required for virulence factor production and is attenuated in numerous animal models including SSTIs (*24*). Given the above results, we infected untreated and STZ-treated mice with wild-type (WT) LAC and the LAC *agr*A::Tn, and consistent with other studies, we show that the *agrA*::Tn strain is attenuated in normal mice in terms of weight loss, lesion size, bacterial burden in the skin, and dissemination to peripheral organs (Fig. 2, D to F, and fig. S4, A to C). We also show that the *agrA*::Tn strain is attenuated compared with WT in hyperglycemic STZ-treated mice, as there is no lesion formation with the *agrA*::Tn (Fig. 2D and fig. S4, D to F). This is despite the increased bacterial burden observed in the skin of the STZ-treated mice infected

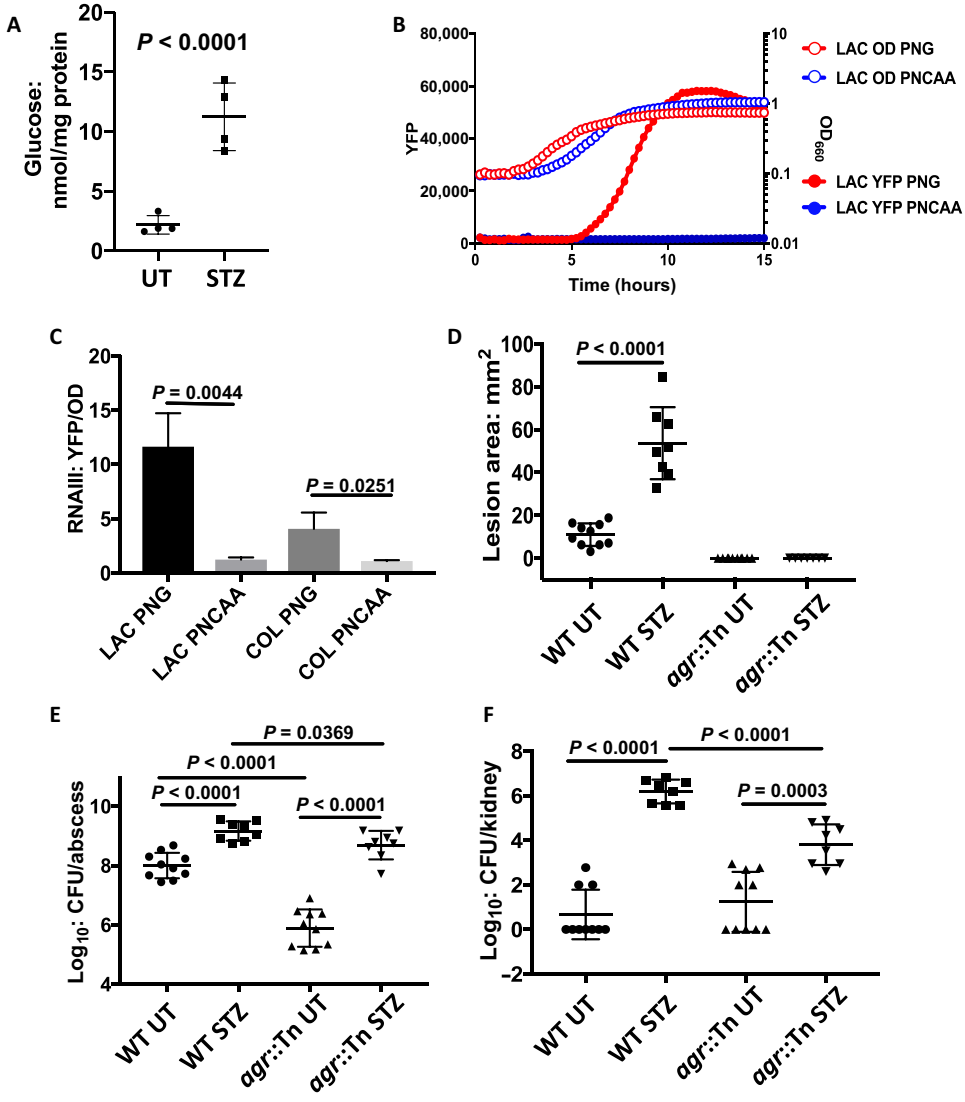

Fig. 2. Agr is required for invasive infections in hyperglycemic mice and requires glucose for activation. Glucose levels were measured in abscesses from untreated and STZ-treated animals and normalized to protein levels. (**A**) Abscesses from STZ-treated animals had significantly higher glucose levels than those from untreated animals. (**B**) *S. aureus* strain LAC harboring a plasmid with YPF linked to the RNAIII promoter (filled symbols) were grown in PNG (red symbols) or PNCAA (blue symbols). Fluorescence is only observed in strains grown in PNG (left axis) (B). (**C**) Relative RNAIII:YFP fluorescence normalized to OD_{660} at 10 hours shows greater induction of RNAIII in strains LAC and COL grown in PNG ($n = 3$). Normal ($N = 9$ and $N = 11$) and diabetic ($N = 11$ and $N = 8$) mice were infected with 1×10^7 CFU of the USA300 MRSA strain LAC or LAC *agr*::Tn ($n = 10$ for untreated and $N = 8$ for STZ-treated). (**D**) Neither treated nor STZ-treated mice infected with *agr*::Tn formed necrotic lesions. (**E**) The *agr*::Tn abscesses had lower bacterial burdens than WT-infected mice in both untreated and STZ-treated mice; however, the reduced burden in STZ-treated mice was not as notable. (**F**) STZ-treated mice infected with *agr*::Tn had significantly less dissemination to the kidneys compared with STZ-treated mice infected with WT LAC.

with *agrA*::Tn (Fig. 2E). The increased burden in STZ-treated animals likely stems from the immune dysregulation and weak oxidative/nitrosative burst described in Fig. 1 and by others (*7*, *9*).

Several virulence factors have been shown to directly contribute to disease severity in murine SSTI models including alpha toxin (Hla) and a myriad of secreted proteases. Hla is known to be responsible for the majority of dermonecrosis associated with *S. aureus* SSTIs (*25*). In addition, in an SSTI, *S. aureus* grows in a biofilm-like aggregate that, in STZ-treated mice, is consistently able to disseminate to peripheral organs. The proteases produced by *S. aureus* potentiate biofilm dispersal, with aureolysin being the most active (*26*). We used a Δ*hla* mutant and an isogenic mutant that lacked all protease production (ΔPro) to determine the contribution of each to invasive infection in hyperglycemic mice. Mice infected with Δ*hla* had decreased lesion size and decreased dissemination to peripheral organs in both untreated and STZ-treated mice as compared with the WT-infected counterparts (fig. S5, A to F). While Δ*hla* exhibited marked reduction in abscess burden in untreated mice, it was still able to reach the elevated burdens of WT infections in the STZ-treated animals (fig. S5C). Unlike the Δ*hla* mutant, the ΔPro mutant was not attenuated in lesion size or abscess burden in untreated mice; however, ΔPro was attenuated in STZ-treated mice, as it produced smaller lesion sizes and decreased dissemination compared with WT-infected mice despite normal bacterial burdens (fig. S5, A to F). The increased bacterial burden observed in the skin of STZ-treated mice infected with the Δ*hla*, ΔPro, and the *agrA*::Tn can most likely be attributed to immune deficiency associated with the lack of insulin signaling. However, these data suggest that hyperglycemic STZ-treated mice are not completely permissive to invasive *S. aureus* infection in that full disease severity and dissemination require virulence factors under the control of Agr.

Glycolysis is required for maximal ATP generation and *S. aureus* virulence factor production

S. aureus grown in chemically defined media supplemented with glucose (PNG) preferentially activated RNAIII transcription compared with media supplemented with casamino acids (PNCAA) (Fig. 2B). In addition to increased RNAIII transcript in PNG, we observed an elevated transcription of *hla*, *psmα*, and *aur* in *S. aureus* grown in PNG and overproduction of Hla secreted into the media (Fig. 3, A and B, and fig. S6, B to D). The mere presence of glucose, however, is not enough to maximize virulence factor production. Mutants unable to efficiently use glucose consistently exhibited reduced *hla* expression. The glycolytic mutants Δ*pfkA* and Δ*pyk* exhibited reduced Hla excretion despite the presence of glucose (Fig. 3, D and E). In addition, mutants with complete and partial defects in converting glucose to glucose-6-phosphate (*ptsH*^{H15A}/*glcK* and *ptsH*^{H15A}, respectively; fig. S6) also produced significantly less Hla and were severely attenuated in both untreated and STZ-treated mice (fig. S7). *ptsH*^{H15A} is an allele that cannot import any carbohydrates via any PTS system but is still able to engage carbon catabolite protein A (CcpA) for carbon catabolite regulation. The mutant can still use glucose via the non-PTS GlcU permease, but this requires glucose kinase (GlcK) to generate glucose-6-phosphate in order for carbon to enter into upper glycolysis (fig. S6).

The mechanism behind the glucose-stimulated virulence factor production in *S. aureus* has never been formally defined. However, given the reduced affinity of AgrC for ATP (K_M = ~1.5 mM, ~1 order of magnitude above other histidine kinases), phosphorylation of AgrA would require high intracellular ATP levels (*18*). Our results show that *S. aureus* grown in PNG contain roughly twice as much intracellular ATP compared with the PNCAA grown counterparts (Fig. 3C). We determined that intracellular ATP concentrations in PNG range between 0.8 and 1 mM, just under the K_M of AgrC for ATP, suggesting that further reduction in ATP pools (e.g., growth in PNCAA) may significantly hinder Agr activity. In further support of the role of ATP levels in modulating toxin production, reducing the efficiency of ATP generation from glucose catabolism also reduced virulence factor expression. In the presence of glucose and oxygen, *S. aureus* uses overflow metabolism where glucose is primarily metabolized to acetate (fig. S4). This pathway provides *S. aureus* the ability to rapidly generate two additional ATP per glucose molecule. *S. aureus* uses the phosphotransacetylase (Pta)–acetate kinase (AckA) pathway to generate acetate and ATP (fig. S6) (*27*). Although not as marked as Δ*pfkA* or Δ*pyk*, our results show that compared with WT, growth of the Δ*ackA* mutant in PNG resulted in less ATP production and decreased Hla production compared with WT (Fig. 3, G to I). Thus, despite being able to fully catabolize glucose, the decreased energy yield in the Δ*ackA* mutant reduced Agr activity, resulting in decreased disease severity in both euglycemic and hyperglycemic animals (Fig. 3, K and L, and fig. S8). Agr activity in the form of Hla excretion was linearly correlated with the level of intracellular ATP in all of the mutants tested [coefficient of determination (R^2) = 0.7], suggesting that Agr activity is tightly linked with the energy state of the cell (Fig. 3J).

Excess glucose in hyperglycemic infections disproportionately potentiates *S. aureus* virulence over fitness

Phlorizin is a competitive inhibitor of the sodium/glucose co-transporters 1 and 2 (SGLT 1 and 2) in the kidney and lowers blood glucose levels by inhibiting glucose reabsorption. We treated mice with phlorizin 1 day before and throughout infection with *S. aureus*. Phlorizin treatment reduced blood glucose to below 200 mg/dl in 7 of 10 treated mice. The phlorizin-treated mice with lower blood glucose had markedly smaller lesion sizes and lower organism burdens and exhibited reduced dissemination to peripheral organs than their hyperglycemic (STZ alone treated) counterparts (Fig. 4, A to F). In addition, using quantitative real-time polymerase chain reaction (PCR), we show that transcripts of *hla*, *psmα*, and *aur* are significantly elevated in hyperglycemic infections compared with untreated controls (Fig. 4G). However, in phlorizin-treated animals, we observe that transcripts of *hla*, *psmα*, and *aur* are reduced to levels observed in euglycemic untreated mice (Fig. 4G). This suggests that the stark reduction in disease severity in phlorizin-treated mice is incongruent with the mere ~half-log reduction in organism burden, despite being statistically significant. Rather, the improved infection outcome from phlorizin treatment results partly from the reversal of excessive virulence factor production in hyperglycemic mice.

Evolutionarily acquired glucose transporters are essential for full toxin production and virulence potential in diabetic mice

In further support of the notion that the primary effect of excess glucose in diabetic infections is to exacerbate virulence factor production, we infected untreated and STZ-treated animals with an *S. aureus* mutant devoid of glucose transport. Unlike Δ*pfkA* or Δ*pyk* mutants, which cannot use any carbohydrate, the ΔG4 mutant

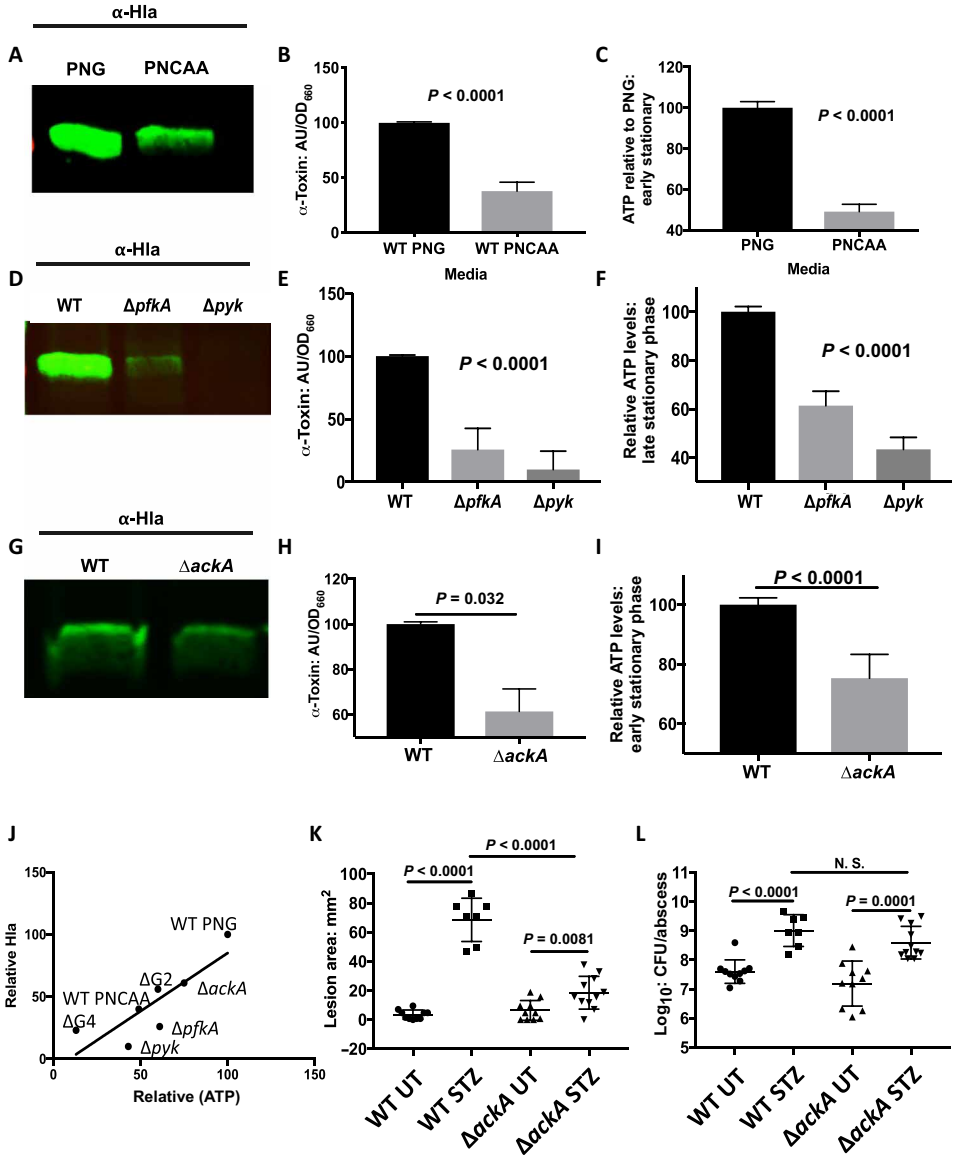

Fig. 3. Toxin production by *S. aureus* requires ATP generation from glycolysis. (**A**) Representative Western blot showing Hla in spent media from LAC grown in PNG (left) or PNCAA (right). (**B**) Quantification of Hla normalized to OD_{660} in LAC grown in PNG or PNCAA ($n = 3$). AU, arbirtrary unit. (**C**)Quantification of intracellular ATP normalized to OD_{660} relative to LAC grown in PNG versus PNCAA ($n = 3$). (**D**) Representative Hla Western blots from culture supernatants from LAC (left), LAC Δ*pfkA* (center), and LAC Δ*pyk* (right) grown in PNMix. (**E**) Quantification of Western blots from LAC, LAC Δ*pfkA*, and LAC Δ*pyk* ($n = 3$). (**F**) Quantification of intracellular ATP normalized to OD_{660} relative to LAC. (**G**) Representative Hla Western blots of culture supernatant from LAC (left) and LAC Δ*ackA* (right) grown in PNG. (**H**) Quantification of α-toxin Western blots from LAC and LAC Δ*ackA* ($n = 3$). (**I**) Quantification of intracellular ATP normalized to OD_{660} relative to LAC ($n = 3$). (**J**) Regression analysis revealed a significant correlation between normalized intracellular ATP and the amount of normalized excreted Hla ($R^2 = 0.7$, nonzero slope, $P = 0.019$). Untreated and STZ-treated mice were infected with 10^7 CFU of WT LAC or LAC Δ*ackA* (WT UT, $n = 10$; WT STZ, $n = 7$; Δ*ackA* UT, $n = 10$; and Δ*ackA* STZ, $n = 11$). (**K**) Untreated mice infected with WT or Δ*ackA* have similar lesion sizes. STZ-treated mice infected with Δ*akcA* have significantly larger lesion sizes than similarly infected untreated mice, but smaller lesion sizes than STZ-treated mice infected with WT (K). (**L**) STZ-treated mice infected with WT have significantly increased bacterial burden in the subcutaneous abscess compared with similarly infected untreated mice. STZ-treated mice infected with Δ*ackA* have significantly increased bacterial burden in the subcutaneous abscess compared with similarly infected untreated mice (L). There is no significant difference in abscess burden in STZ-treated mice infected with WT or Δ*ackA* (L). N.S., not significant.

(lacking all four glucose transporters: *glcA*, *glcB*, *glcC*, and *glcU*) is specifically defective in glucose utilization (*12*). We observed decreased ATP levels concomitant with decreased Hla accumulation in media and decreased transcript levels of *hla*, *psm*-α, and *aur* when ΔG4 was grown in CDM with both glucose and casamino acid carbon/energy sources (PNMix) (Fig. 5, A to D). This translates into markedly reduced lesion sizes and dissemination to peripheral organs in both untreated and STZ-treated animals (Fig. 5, F and G, and fig. S9). Even at day 3, when abscess sizes are largest, we see no observable skin lesion in ΔG4-infected STZ-treated animals (fig. S9E). Again, this decreased disease severity cannot be fully explained by reduced organism burdens, particularly in the case of hyperglycemic animals in which the ΔG4 was still overabundant by ~2-logs compared with untreated mice (Fig. 5G). Rather, real-time PCR performed on

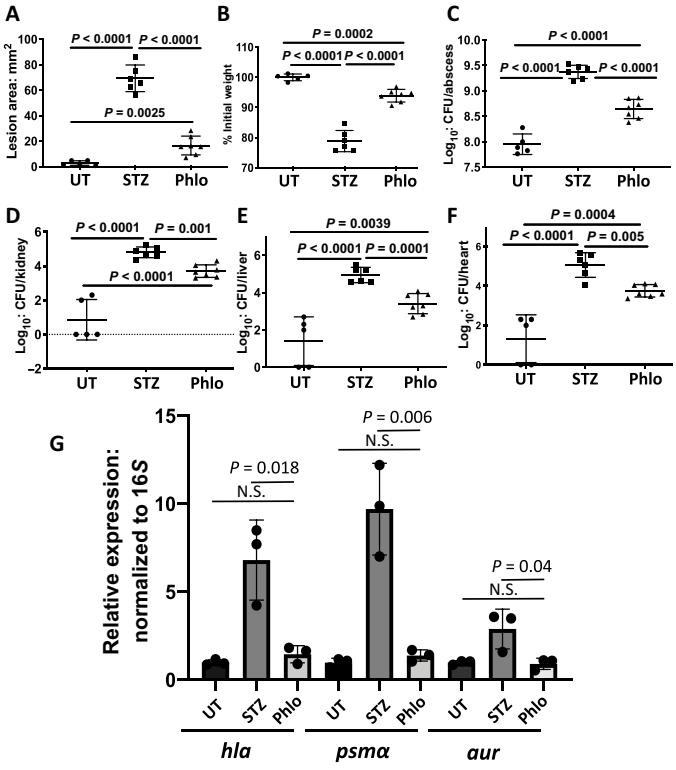

Fig. 4. Reducing blood glucose in hyperglycemic mice with phlorizin reverses infection severity. Mice were treated with phlorizin (Phlo) 1 day before infection and throughout the course of infection to lower blood glucose levels without influencing insulin signaling. (**A**) STZ-treated mice treated with phlorizin had smaller lesions than mice treated with STZ alone, but larger lesions than untreated mice. (**B**) Infected STZ-treated mice display significant weight loss that is reversed with phlorizin. (**C**) STZ-treated mice that were further treated with phlorizin display lower abscess burdens than mice treated with STZ-alone, but higher burdens than untreated mice. Phlorizin treatment resulted in decreased dissemination to the peripheral organs in STZ-treated mice including the kidneys (**D**), liver (**E**), and heart (**F**). (**G**) Quantitative real-time PCR *S. aureus* isolated from untreated, STZ-treated, and dual STZ phlorizin abscesses showed significantly increased expression ($P < 0.05$) of *hla*, *psmα*, and *aur* in STZ-treated mice that is reversed by phlorizin.

WT and ΔG4 isolates from hyperglycemic abscesses showed markedly decreased transcription of *hla*, *psm*-α, and *aur* in the ΔG4 strain (Fig. 5E). Thus, mutants that are unable to capitalize on excess blood glucose in hyperglycemic tissue cause markedly reduced disease severity with only a modest reduction in organism burden.

Glycolysis is essential for both the full virulence capacity of *S. aureus* and the ability of the host to mount an effective immune response against invading pathogens. Consequently, the host uses two dedicated, high-affinity glucose transporters (GLUT-1 and GLUT-3) to support active inflammatory phagocyte activity. Similarly, two of the four *S. aureus* glucose transporters, GlcA and GlcC, are recent additions to the genome, as they are absent in all but two other staphylococcal species and overly contribute to glucose transport (Fig. 6A) (*12*). We deleted *glcA* and *glcC* (ΔG2) to determine the contribution of these recently acquired, highly active glucose transporters to *S. aureus* toxin production and virulence. Although not as robust as the ΔG4 mutant, the ΔG2 mutant had decreased intracellular ATP levels and decreased Hla production (Fig. 5, A to C). The ΔG2 mutant was moderately attenuated in untreated euglycemic mice but achieved WT levels of abscess burden hyperglycemic abscesses (Fig. 6C). However, STZ-treated mice infected with ΔG2 exhibited decreased weight loss, smaller lesion sizes, and reduced dissemination compared with WT infections (Fig. 6, B to D, and fig. S10). Thus, for *S. aureus* to fully benefit from elevated blood glucose in hyperglycemic animals, it must express these two newly acquired, highly active glucose PTS systems.

DISCUSSION

Individuals with diabetes are prone to more frequent and invasive SSTIs, with *S. aureus* being the most common pathogen isolated from diabetic wounds (*2*, *4*, *28*). Previous studies have proposed that decreased respiratory burst produced by innate immune cells might be the underlying cause of increased infection severity; however, the mechanisms for suppressed immunity are not known (*7*–*9*). Upon stimulation, infiltrating phagocytes adopt a metabolic strategy whereby high glycolytic flux is redox balanced via lactate production. The excess requirement for glucose acquisition is met by the induction of high-affinity glucose transporters, GLUT-1 and GLUT-3, on infiltrating phagocytes (Fig. 1H and fig. S2A) (*21*). The ability to transition into this metabolic state is critical for immune output since any interference with phagocyte glucose import precludes an effective oxidative burst and bacterial clearance (figs. S2, C and D, and S3, E and F) (*20*). We previously showed that *S. aureus* has evolved a similar metabolic strategy through the genetic acquisition of two highly active glucose transporters (*glcA* and *glcC*; Fig. 6A and fig. S6A) and a highly active lactate dehydrogenase (*ldh*1) to resist immune radicals such as NO (*12*). This "metabolic mimicry" affords *S. aureus* the ability to thrive at sites of inflammation, provided that it has adequate access to glucose. However, over time, the supply of glucose is diminished by the ever-increasing populations of infiltrating phagocytes, eventually leading to the resolution of the SSTI and bacterial clearance (Fig. 1, A to C) (*29*). In STZ-treated hosts, however, this coordinated immunometabolic response is completely dysfunctional, as infiltrating phagocytes do not express GLUT-1 or GLUT-3 and do not elicit a respiratory burst (Fig. 1, F to H, and fig. S2, A and B). The lack of robust immune radical production has been previously observed in multiple diabetic models of infection; however, a role in glucose transport was never implicated. In addition, we observed a sixfold increase in glucose in abscesses from STZ-treated animals compared with those from untreated mice even though there is only about a fourfold increase in blood glucose (Fig. 2A). This suggests that competition for glucose at the infection site is another form of nutritional immunity reminiscent of the host scavenging transition metals such as iron, zinc, and manganese, all of which have been shown to directly contribute to *S. aureus* clearance in resolving SSTIs (*30*, *31*). Moreover, only people with diabetes that have poor glycemic control [HB1Ac (glycated hemoglobin) > 8.5] are at a heightened risk for developing severe MRSA SSTIs, suggesting that sustained hyperglycemia is a driving force in infection susceptibility (*32*). This raises the question of how decreased nutritional immunity and the concomitant increase in tissue glucose contribute to invasive infection in diabetic SSTIs.

The Agr system controls the expression of several *S. aureus* virulence factors and requires glucose for activation (Fig. 2, B and D). The sensor kinase AgrC belongs to the HPK-10 family of histidine kinases with variations at key conserved Asp residues. The Asp to

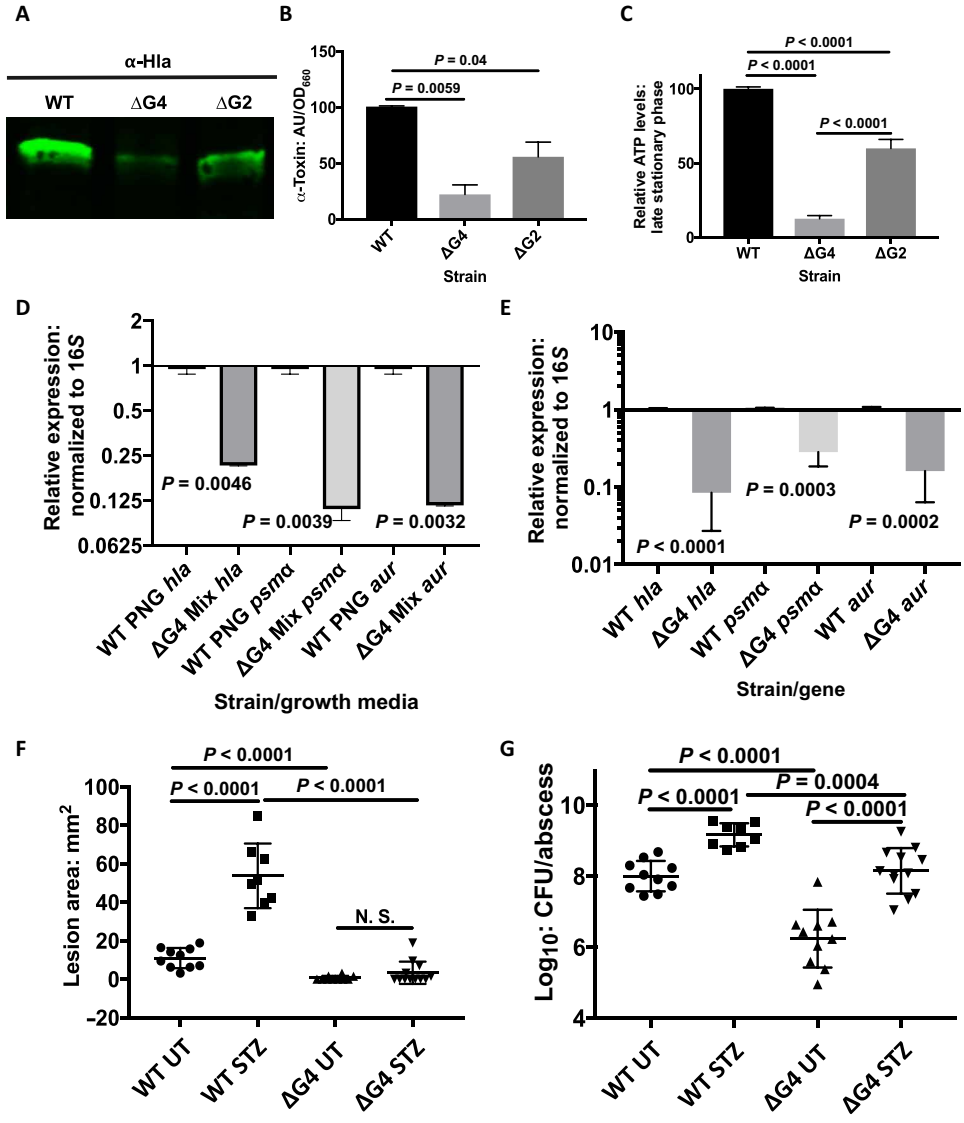

Fig. 5. Glucose transporters are essential for ATP and toxin production. (**A**) Representative Hla Western blot from supernatants of WT LAC, LAC ΔG4 (lacking all glucose transporters), and LAC ΔG2 (lacking the recently acquired GlcC and GlcA transporters) grown in PNG. (**B**) Quantification of Hla Western blots ($n = 3$) showing significantly decreased Hla production by LAC ΔG2 and LAC ΔG4 compared to WT LAC. (**C**) The LAC ΔG4 (lacking all glucose transporters) and LAC ΔG2 have reduced intracellular ATP compared to WT LAC when grown in PNG. (**D**) Quantitative real-time PCR from WT LAC and LAC ΔG4 grown in PNG shows significant decreases in *aur*, *psmα*, and *hla* transcripts in LAC ΔG4 ($n = 3$). (**E**) Quantitative real-time PCR from WT LAC and LAC ΔG4 isolated from STZ-treated mice showed reduced transcript levels of *hla*, *psmα*, and *aur* in LAC ΔG4. (**F**) Day 7 lesion sizes measured from untreated mice infected with LAC ΔG4 were virtually undetectable, and abscesses in STZ-treated mice infected with LAC ΔG4 also rarely had small lesions. (**G**) LAC ΔG4 is attenuated in untreated and STZ-treated mice compared with WT LAC but has higher CFU in STZ-treated animals.

Asn variation results in roughly a 10-fold reduction in affinity toward ATP for AgrC compared with other families of two-component systems (*18*). The K_M for canonical histidine kinases is well below the intracellular ATP concentrations found in all conditions tested here (K_M = ~100 μM range), and therefore, activity would not be affected by the energy state of the cell. In contrast, the low affinity of AgrC toward ATP allows for the coordination of cell density signals with that of the energy state of the cell. Given that *S. aureus* has evolved to maximize energy production via glycolysis, this links Agr activity to the availability of glucose, which is overly abundant in the abscesses of STZ-treated animals (Fig. 2A). However, linking Agr activity to the availability of an organism's preferred energy source may be important for proper responses to stimuli by HPK-10 family members beyond virulence, as many are found in nonpathogenic bacteria.

In an SSTI, *S. aureus* grows in a biofilm-like aggregate that is able to disseminate to peripheral organs in STZ-treated mice. Our results show that STZ-treated mice develop more severe infections by every measurable metric and that this phenotype requires the Agr TCS (Fig. 2, D to F, and fig. S4). Agr-regulated proteases and Hla contribute equally to invasive infection in diabetes. The expression of proteases, primarily aureolysin, is essential for *S. aureus* biofilm dissemination, while Hla is required for SSTI lesion formation (fig. S3). In hyperglycemic mice, the *hla* mutant was more attenuated in lesion formation than the protease mutant, but both mutants were

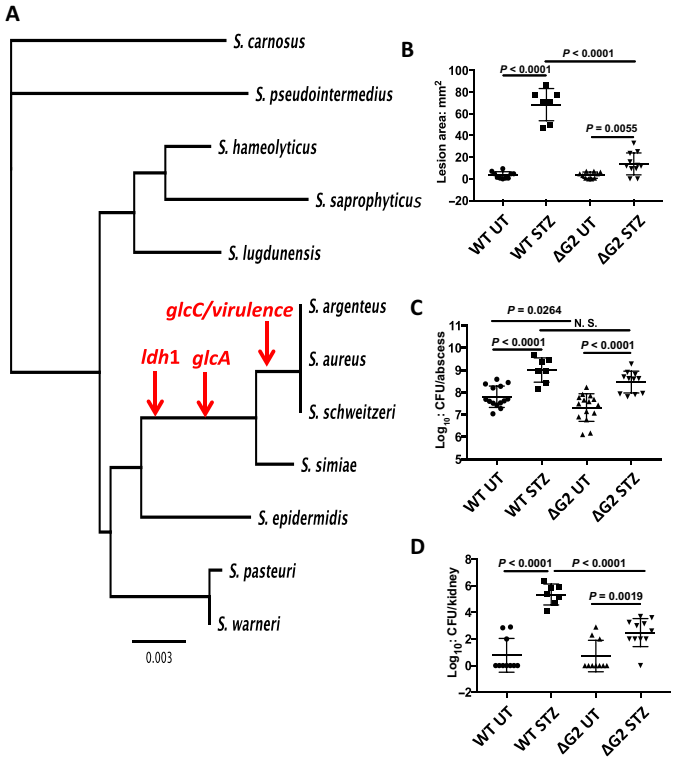

Fig. 6. The evolutionary acquisition of glucose transporters by *S. aureus* coincides with acquisition of virulence factors. A phylogenetic tree based on 16*S* ribosomal DNA sequences showing the relation of *S. aureus* to other staphylococcal species. Red arrows show where *S. aureus* and other related species evolutionarily acquired lactate dehydrogenase 1 (*ldh1*), glucose transporter A (*glcA*), glucose transporter C (*glcC*), and virulence factors including α-, β-, and γ-hemolysins (**A**). Untreated and STZ-treated mice were infected with 1×10^7 CFU of WT and ΔG2 (WT UT, $n = 10$; WT STZ, $n = 7$ to 8; ΔG2 UT, $n = 10$; and ΔG2 STZ, $n = 11$). STZ-treated mice infected with WT had larger lesion sizes than infected untreated mice. STZ-treated mice infected with ΔG2 had smaller lesion sizes than WT infected STZ-treated mice (**B**). (**C**) STZ-treated mice infected with WT or ΔG2 had significantly higher abscess bacterial burdens than their untreated infected controls. (**D**) STZ-treated mice infected with WT displayed increased dissemination to the kidneys compared to similarly infected untreated mice. STZ-treated mice infected with ΔG2 had increased dissemination to the kidneys compared to similarly infected untreated mice (D).

similarly attenuated in dissemination (fig. S5). During the course of an SSTI, the host generates an abscess wall consisting of mostly collagen and fibronectin around the infected tissue. This creates an environment devoid of glucose while simultaneously preventing the spread *S. aureus* to neighboring tissues (*29*). Since collagen is one of the substrates readily hydrolyzed by Aur, one could envision in a hyperglycemic SSTI that the overabundant expression of proteases would continually degrade the primary components of the abscess wall while simultaneously promoting dissemination of the biofilm-like aggregate. Moreover, increased Hla expression accelerates dermonecrosis and lesion growth, thereby preventing the host from properly walling off the abscess. This scenario potentially explains why both Hla and proteases are necessary for invasive infection in STZ-treated mice.

We contend that immune dysfunction in STZ-treated animals primarily results in increased bacterial burdens, whereas elevated tissue glucose is responsible for increased *S. aureus* virulence factor production. For instance, ΔG4 mutants are still able to attain nearly the same elevated skin burdens in STZ-treated mice given their inherent immune dysfunction. However, the ΔG4 mutant does not cause lesions or disseminate since it cannot capitalize on the excess tissue glucose in hyperglycemic SSTIs (Fig. 5, F and G, and fig. S9, B to D). We also observe a similar phenotype with the Agr mutant in that bacterial numbers increase in abscesses from STZ-treated mice, but there is no corresponding increase in dermonecrosis or dissemination (Fig. 2, D to F) Furthermore, phlorizin treatment, which lowers blood glucose without restoring insulin signaling or full immune function, completely abrogated excessive virulence factor production and significantly reduced abscess lesion area without lowering organism burdens by even a log (Fig. 4). Thus, the diabetic state results in two deficiencies that directly affect the outcome of *S. aureus* SSTIs: reduced immune output that allows for bacterial overgrowth and limited nutritional immunity resulting in excess glucose, which directly stimulates Agr-dependent virulence.

The recent acquisition of the glucose transporters GlcA and GlcC significantly contributes to *S. aureus* virulence, particularly in hyperglycemic tissues (Fig. 6, B to D, and fig. S10, F to H). These two PTS transporters are highly active and support the ability of *S. aureus* to battle the host's nutritional immunity strategy, at least for a while before the increasing immune infiltrate overwhelms the competitive abilities of invading bacteria. In STZ-treated animals, a ΔG2 mutant, which has the same glucose transport ability of *Staphylococcus epidermidis*, cannot take advantage of the excess tissue glucose and largely resembles an infection with a ΔG4 mutant completely devoid of glucose transport. Furthermore, the most recent acquisition of GlcC coincided with the acquisition of several toxins including α-, β-, and γ-hemolysins (Fig. 6A). *Staphylococcus schweitzeri* and *Staphylococcus argenteus* both have *glcA* and *glcC* as well as all three hemolysins and several proteases (Fig. 6A). In contrast, *Staphylococcus simiae* lacks *glcC* and does not encode any hemolysins or nearly as many proteases. Not much is known about *S. schweitzeri*, but *S. argenteus* was initially classified as *S. aureus* until further analysis revealed it to be a unique species (*33*). Furthermore, *S. argenteus* is an emerging pathogen in Southeast Asia with several isolates coming from patients with diabetes (*34*). Whether metabolic evolution preceded or succeeded the acquisition of virulence is still unknown. However, the correlation of the two supports the role of host glucose as a signal to *S. aureus* that it is no longer on the skin surface (where carbohydrates are scarce), but rather in deeper tissue replete with serum glucose. Consequently, this signal results in the pathogen modulating both virulence and metabolism. Moreover, two other Gram-positive pathogens that are readily killed by immune radicals, *Streptococcus pyogenes* and *Enterococcus* spp., are associated with invasive infections in patients with diabetes (*28*). Much like *S. aureus*, both of these pathogens link glucose availability to virulence factor production (*35*, *36*). This suggests that several organisms that cause invasive infections in people with severe diabetes are evolutionarily predisposed to take advantage of immune suppression and the availability of excess glucose (*35*, *36*).

The reasons why people with diabetes are prone to more frequent and invasive infections have remained elusive. One obvious reason for increased infection frequency in individuals with diabetes is immune suppression, as several commensal bacteria are frequently isolated from diabetic wounds but do not cause invasive infections. Here, we show that the lack of GLUT-1/-3 expression on infiltrating phagocytes from STZ-treated, insulin-deficient animals correlates

with their inability to mount an effective oxidative burst and clear the infection. However, the mechanism explaining the requirement of effective insulin signaling for phagocyte GLUT-1/-3 expression remains unknown. That said, we can now begin to understand why patients with diabetes suffer specifically from *S. aureus* infections so frequently. Our results show that the evolutionary coupling of expanded glycolytic capacity with toxin production in *S. aureus* and suppressed host nutritional immunity allows this pathogen to take advantage of the unique infection environment associated with advanced diabetes, resulting in more severe infections. Furthermore, these data suggest that the development of specific inhibitors of bacterial glycolytic enzymes would be beneficial for treating infections in people with diabetes (*37*).

Contact for reagent and resource sharing

Further information and requests for resources and reagents should be directed to and will be fulfilled by the lead contact, A. R. Richardson (anthony.richardson@pitt.edu).

MATERIALS AND METHODS

Bacterial strains and growth conditions

The bacterial strains used in this study are listed in the core resource table. *S. aureus* strain LAC was used in in vitro and in vivo studies. *S. aureus* was grown in the brain heart infusion (BHI) for mouse infection studies. For in vitro studies, *S. aureus* was grown in CDM supplemented with glucose (PNG), casamino acids (PNCAA), or both (PNMix) at 37°C with shaking at 250 revolutions per minute (rpm) as previously described (*38*). Bacteria were enumerated by plating for viable CFUs on BHI agar plates.

Animal studies

Animal experiments were approved by the University of Pittsburgh Animal Care and Use Committee (protocol nos. 16027663 and 15127428). Investigators were not blinded, and studies were not randomized. No statistical method was used to predetermine sample size. C57BL/6J mice were obtained from Jackson Labs (Bar Harbor, ME). Mice were maintained on a 14-hour light cycle and housed five mice per cage. Mice were checked daily during infection studies. Veterinary care was provided 7 days a week. Studies used female mice between 8 and 12 weeks old.

Quantitative real-time reverse transcription PCR

Infected abscesses were carefully dissected and were homogenized in 500 μl of TRIzol reagent (Ambion, Carlsbad, CA). Total RNA was purified from homogenates using a PureLink RNA mini kit (Invitrogen, Carlsbad, CA) following the manufacturer's directions. Quantitative real-time reverse transcription (RT) PCR was performed with a SensiFAST SYBR no-ROX one-step kit (Bioline, Taunton, MA) using 50 ng of RNA/reaction and primers psma forward (TATCAAAAGCTTAATCGAACAATTC), psma reverse (CCCCTTAAATAAGATGTTCATATC); Hla forward (ACAATTTTAGAGAGCCCAACTGAT); Hla reverse (TCCCCAATTTTGATTCACCAT); 16*S* forward (TCATCCTGGCTCAGGATGA); 16*S* reverse (TTCGCTCGACTTGCATGTA); Aur forward (GTGATGGTGATGGTCGCACATTC); and Aur reverse (GCGTAAAGCGTCTCCCTCTTTTC). Reaction conditions were specified by Bioline and performed with a MyIQ thermocycler (Bio-Rad, Indianapolis, IN). All transcript levels were normalized to 16*S*.

Western blot

Western blots for α-hemolysin were performed on clarified culture supernatants. Cultures were grown in the appropriate CDM to an $OD_{660} \approx 5.0$, and a 1-ml volume of culture was removed for analysis. A 20-μl aliquot of culture was used for bacterial enumeration by dilution plating. Supernatants were clarified by centrifugation at 12,000 rpm for 5 min. Clarified supernatants were boiled, and ≈30 μl was loaded on a 12% SDS polyacrylamide gel and subsequently transferred to a nitrocellulose membrane. Membranes were blocked using LI-COR blocking buffer (LI-COR, Omaha, NE) and probed with anti–α-hemolysin antibody (Abcam, Cambridge, MA) overnight at 4°C. Membranes were washed and incubated with IRDye 800CW secondary antibodies (LI-COR). Membranes were imaged using a LI-COR Odyssey infrared imager, and band densities were quantified using Image Studio version 4.0 (LI-COR). Band intensities were normalized to CFU.

Mouse infections

Diabetic mice were generated by intraperitoneal injection of STZ (Sigma-Aldrich) at a dose of ≈225 mg/kg. Mouse blood glucose was analyzed 3 days after STZ treatment using a glucometer. Only mice with a blood glucose level >300 mg/dl were used as hyperglycemic mice. Mice that did not become hyperglycemic following STZ administration were not used for further studies. For the phlorizin studies, phlorizin was administered twice daily at 400 mg/kg (in 10% ethanol, 15% dimethyl sulfoxide, and 75% saline) by subcutaneous injection on the flank of the mouse without infection. Phlorizin was administered 1 day before infection and every day through the course of infection. Mice that had blood glucose levels about 300 mg/dl after phlorizin treatment were not included in subsequent analysis. Subcutaneous infections were performed as previously described (*39*). Bacteria were grown overnight in BHI, washed 3× with phosphate-buffered saline (PBS), and enumerated by dilution plating. Washed bacteria were stored overnight in PBS at 4°C. Bacteria were subsequently adjusted to a concentration of 5×10^8 in PBS, allowing for a 20-μl injection to equal 1×10^7 CFU. Mice were anesthetized with 2,2,2-tribromoethanol followed by shaving of the left flank. *S. aureus* in 20 μl was injected subcutaneously at $\approx 1 \times 10^7$ CFU. Mice were euthanized on day 7 after inoculation, and tissues were collected for glucose content, RNA isolation, or bacterial enumeration.

Glucose quantification

Abscess tissues were carefully dissected away from healthy tissues and were homogenized in 500 μl of radioimmunoprecipitation assay buffer (Boston BioProducts). Abscess homogenates were subsequently centrifuged twice at 12,000*g* for 15 min, and protein content from the clarified supernatants was quantified using a bicinchoninic acid assay (Thermo Fisher Scientific). Glucose from clarified supernatants containing equivalent amounts of protein was quantified using the glucose assay kit from EMD Millipore (Billerica, MA) following the manufacturer instructions.

Quantification and statistical analysis

Statistical method and sample size (*n*) are indicated in the figure legends. For in vivo studies, *n* represents the number of mice or tissues per group. For in vitro studies, *n* represents the number of biological replicates. Statistical analysis was performed using Prism 7 (GraphPad) software. A two-tailed Student's *t* test was performed on the means of

all parametric data. Statistical significance was defined as $P < 0.05$. Error bars on figures show SEM.

Intracellular ATP assays

Cultures grown (5 ml) to an OD_{660} of interest in PN + carbon source (0.5% glucose, 1% casamino acid, or a mix of glucose and CAA). Strains were washed three times in PBS and diluted 1:100. Intracellular ATP concentrations were determined using a Promega BacTiter-Glo assay kit (Promega Corporation, Madison, WI) following the manufacturer's instructions. Sample luminescence was determined using a Synergy H1 microplate reader (BioTek, Winooski, VT).

YFP reporter

RNAIII-YFP promoter fusion was previously described (*40*). Samples were inoculated in indicated media, and growth curves were generated on a Tecan Infinite M200 (software, Magellan V7.2). Samples were shaken with amplitude of 1, continuously at 37°C, read every 15 min, OD_{660} (no. of flashes, 25), YFP emission at 485, excitation at 535, and gain at 100. Graphs were generated using Prism 7.

Immunohistochemistry

IHC was performed on tissues as previously described (*41*). In brief, abscess tissues were fixed in 10% formalin, paraffin embedded, sectioned (10 μm), and stained with hematoxylin and eosin by the University of North Carolina Histopathology Core Facility or by the histology lab facility in the McGowan Institute for Regenerative Medicine at the University Pittsburgh School of Medicine. For immunofluorescence staining, unstained sections were deparaffinized using a graded series of xylene and ethanol washes followed by heat-mediated antigen retrieval for 20 min in 10-mM sodium citrate buffer (pH 6). Specimens were blocked for 1 hour in 10% serum from the host species of the secondary antibody and subsequently incubated overnight with primary antibodies. Primary antibodies against GLUT-1 and GLUT-3 were obtained from Biorbyt (Cambridge, UK). The nitrotyrosine antibody was obtained from Millipore (Temecula, CA). Primary antibodies were detected with the use of biotinylated secondary antibodies followed by incubation with Alexa Fluor 594–conjugated streptavidin (Jackson ImmunoResearch, West Grove, PA). Stained sections were mounted in ProLong Antifade Gold reagent with DAPI (Invitrogen, Grand Island, NY). Samples were viewed with an Olympus BX60 fluorescence microscope. iVision Software v.4.0.0.0 (BioVision Technologies, New Minas, Nova Scotia) was used for image collection.

Macrophage assays

RAW 264.7 macrophages were suspended in RPMI 1640 (catalog no. 11875-093; Gibco) supplemented with fetal bovine serum (FBS) (10%) and at a concentration of 1×10^6 cells/ml, seeded into the wells of a 48-well plate at 0.5 ml per well, and incubated for 18 hours at 37°C. The cells were then activated via incubation in RPMI 1640 plus lipopolysaccharide (LPS) (100 ng/ml) and interferon-γ (IFN-γ) (20 ng/ml) for 1 hour at 37°C and then spin inoculated in RPMI 1640 alone with *S. aureus* (opsonized in Hanks' balanced salt solution plus 10% mouse serum with active complement at 37°C for 30 min) at a multiplicity of infection of 10:1 (*S. aureus*/RAW 264.7). Following incubation of the RAW 264.7 cells with *S. aureus* for 30 min at 37°C, the cells were washed twice with PBS and then incubated in RPMI 1640 plus gentamicin (100 μg/ml) for 1 hour at 37°C. The infected RAW 264.7 cells were then washed twice with PBS, after which certain wells were treated with 0.01% Triton X-100 to induce RAW 264.7 cell lysis for bacterial enumeration (time zero), while the remaining infected RAW 264.7 cells were incubated in RPMI 1640 plus gentamicin (12 μg/ml) at 37°C for an additional 12 hours. Experiments involving glucose titration used RPMI 1640 without glucose (catalog no. 11879-020; Gibco) that was supplemented with FBS (10%). Oxidative burst was measured using Dihydrorhodamine 123 (DHR) (Cayman Chemical, Ann Arbor, MI). DHR is a cell-permeable fluorogenic probe that measures intracellular peroxynitrite formation. For DHR experiments, RAW 264.7 at a concentration of 2×10^6 cells in 1 ml of media in a six-well plate were incubated for 24 hours at 37°C in the presence or absence of glucose. Following the 24-hour incubation, cells were washed and incubated in fresh media containing LPS (100 ng/ml), IFN-γ (20 ng/ml), and 10 μM DHR for 1 hour. Following incubation, cells were washed three times in PBS and resuspended in 200 μl of PBS in a 96-well plate, and fluorescence was measured using a Tecan Infinite M200 Pro microplate reader following the manufacturer's instructions.

SUPPLEMENTARY MATERIALS

Supplementary material for this article is available at http://advances.sciencemag.org/cgi/content/full/6/46/eabc5569/DC1

View/request a protocol for this paper from *Bio-protocol*.

REFERENCES AND NOTES

1. W. Abu-Ashour, L. Twells, J. Valcour, A. Randell, J. Donnan, P. Howse, J.-M. Gamble, The association between diabetes mellitus and incident infections: A systematic review and meta-analysis of observational studies. *BMJ Open Diabetes Res. Care* **5**, e000336 (2017).
2. W. Abu-Ashour, L. K. Twells, J. E. Valcour, J.-M. Gamble, Diabetes and the occurrence of infection in primary care: A matched cohort study. *BMC Infect. Dis.* **18**, 67 (2018).
3. B. A. Lipsky, Y. P. Tabak, R. S. Johannes, L. Vo, L. Hyde, J. A. Weigelt, Skin and soft tissue infections in hospitalised patients with diabetes: Culture isolates and risk factors associated with mortality, length of stay and cost. *Diabetologia* **53**, 914–923 (2010).
4. J. Smit, M. Søgaard, H. C. Schønheyder, H. Nielsen, T. Frøslev, R. W. Thomsen, Diabetes and risk of community-acquired *Staphylococcus aureus* bacteremia: A population-based case-control study. *Eur. J. Endocrinol.* **174**, 631–639 (2016).
5. J. Jneid, N. Cassir, S. Schuldiner, N. Jourdan, A. Sotto, J. P. Lavigne, B. la Scola, Exploring the microbiota of diabetic foot infections with culturomics. *Front. Cell. Inf. Microbiol.* **8**, 282 (2018).
6. C. W. Farnsworth, E. M. Schott, A. Benvie, S. L. Kates, E. M. Schwarz, S. R. Gill, M. J. Zuscik, R. A. Mooney, Exacerbated *Staphylococcus aureus* Foot Infections in obese/diabetic mice are associated with impaired germinal center reactions, Ig class switching, and humoral immunity. *J. Immunol.* **201**, 560–572 (2018).
7. F. Hanses, S. Park, J. Rich, J. C. Lee, Reduced neutrophil apoptosis in diabetic mice during staphylococcal infection leads to prolonged Tnfα production and reduced neutrophil clearance. *PLOS ONE* **6**, e23633 (2011).
8. K. T. Nguyen, A. K. Seth, S. J. Hong, M. R. Geringer, P. Xie, K. P. Leung, T. A. Mustoe, R. D. Galiano, Deficient cytokine expression and neutrophil oxidative burst contribute to impaired cutaneous wound healing in diabetic, biofilm-containing chronic wounds. *Wound Repair Regen.* **21**, 833–841 (2013).
9. S. Park, J. Rich, F. Hanses, J. C. Lee, Defects in innate immunity predispose C57BL/6J-Leprdb/Leprdb mice to infection by *Staphylococcus aureus*. *Infect. Immun.* **77**, 1008–1014 (2009).
10. D.-F. Zhang, X. Y. Zhi, J. Zhang, G. C. Paoli, Y. Cui, C. Shi, X. Shi, Preliminary comparative genomics revealed pathogenic potential and international spread of *Staphylococcus argenteus*. *BMC Genomics* **18**, 808–817 (2017).
11. H. Suzuki, T. Lefébure, P. P. Bitar, M. J. Stanhope, Comparative genomic analysis of the genus *Staphylococcus* including *Staphylococcus aureus* and its newly described sister species *Staphylococcus simiae*. *BMC Genomics* **13**, 38 (2012).
12. N. P. Vitko, M. R. Grosser, D. Khatri, T. R. Lance, A. R. Richardson, Expanded glucose import capability affords *Staphylococcus aureus* optimized glycolytic flux during infection. *mBio* **7**, e00296-16 (2016).
13. R. P. Novick, E. Geisinger, Quorum sensing in staphylococci. *Annu. Rev. Genet.* **42**, 541–564 (2008).

14. M. Thoendel, J. S. Kavanaugh, C. E. Flack, A. R. Horswill, Peptide signaling in the staphylococci. *Chem. Rev.* **111**, 117–151 (2011).
15. S. Y. Queck, M. Jameson-Lee, A. E. Villaruz, T. H. L. Bach, B. A. Khan, D. E. Sturdevant, S. M. Ricklefs, M. Li, M. Otto, RNAIII-independent target gene control by the agr quorum-sensing system: Insight into the evolution of virulence regulation in *Staphylococcus aureus*. *Mol. Cell* **32**, 150–158 (2008).
16. R. P. Novick, H. F. Ross, S. J. Projan, J. Kornblum, B. Kreiswirth, S. Moghazeh, Synthesis of staphylococcal virulence factors is controlled by a regulatory RNA molecule. *EMBO J.* **12**, 3967–3975 (1993).
17. E. Geisinger, R. P. Adhikari, R. Jin, H. F. Ross, R. P. Novick, Inhibition of rot translation by RNAIII, a key feature of agr function. *Mol. Microbiol.* **61**, 1038–1048 (2006).
18. B. Wang, A. Zhao, R. P. Novick, T. W. Muir, Activation and inhibition of the receptor histidine kinase AgrC occurs through opposite helical transduction motions. *Mol. Cell* **53**, 929–940 (2014).
19. B. Wang, A. Zhao, Q. Xie, P. D. Olinares, B. T. Chait, R. P. Novick, T. W. Muir, Functional plasticity of the AgrC receptor histidine kinase required for Staphylococcal Virulence. *Cell Chem. Biol.* **24**, 76–86 (2017).
20. B. Kelly, L. A. J. O'Neill, Metabolic reprogramming in macrophages and dendritic cells in innate immunity. *Cell Res.* **25**, 771–784 (2015).
21. A. J. Freemerman, A. R. Johnson, G. N. Sacks, J. J. Milner, E. L. Kirk, M. A. Troester, A. N. Macintyre, P. Goraksha-Hicks, J. C. Rathmell, L. Makowski, Metabolic reprogramming of macrophages: Glucose transporter 1 (GLUT1)-mediated glucose metabolism drives a proinflammatory phenotype. *J. Biol. Chem.* **289**, 7884–7896 (2014).
22. M. Bischoff, B. Wonnenberg, N. Nippe, N. J. Nyffenegger-Jann, M. Voss, C. Beisswenger, C. Sunderkötter, V. Molle, Q. T. Dinh, F. Lammert, R. Bals, M. Herrmann, G. A. Somerville, T. Tschernig, R. Gaupp, CcpA affects infectivity of *Staphylococcus aureus* in a hyperglycemic environment. *Front. Cell. Inf. Microbiol.* **7**, 172 (2017).
23. K. Seidl, M. Stucki, M. Ruegg, C. Goerke, C. Wolz, L. Harris, B. Berger-Bächi, M. Bischoff, *Staphylococcus aureus* CcpA affects virulence determinant production and antibiotic resistance. *Antimicrob. Agents Chemother.* **50**, 1183–1194 (2006).
24. E. K. Sully, N. Malachowa, B. O. Elmore, S. M. Alexander, J. K. Femling, B. M. Gray, F. R. DeLeo, M. Otto, A. L. Cheung, B. S. Edwards, L. A. Sklar, A. R. Horswill, P. R. Hall, H. D. Gresham, Selective chemical inhibition of agr quorum sensing in *Staphylococcus aureus* promotes host defense with minimal impact on resistance. *PLOS Pathog.* **10**, e1004174 (2014).
25. A. D. Kennedy, J. B. Wardenburg, D. J. Gardner, D. Long, A. R. Whitney, K. R. Braughton, O. Schneewind, F. R. DeLeo, Targeting of alpha-hemolysin by active or passive immunization decreases severity of USA300 skin infection in a mouse model. *J. Infect. Dis.* **202**, 1050–1058 (2010).
26. A. J. Loughran, D. N. Atwood, A. C. Anthony, N. S. Harik, H. J. Spencer, K. E. Beenken, M. S. Smeltzer, Impact of individual extracellular proteases on Staphylococcus aureus biofilm formation in diverse clinical isolates and their isogenic sarA mutants. *MicrobiologyOpen* **3**, 897–909 (2014).
27. M. R. Sadykov, V. C. Thomas, D. D. Marshall, C. J. Wenstrom, D. E. Moormeier, T. J. Widhelm, A. S. Nuxoll, R. Powers, K. W. Bayles, Inactivation of the Pta-AckA pathway causes cell death in *Staphylococcus aureus*. *J. Bacteriol.* **195**, 3035–3044 (2013).
28. A. Y. Peleg, T. Weerarathna, J. S. McCarthy, T. M. E. Davis, Common infections in diabetes: Pathogenesis, management and relationship to glycaemic control. *Diabetes Metab. Res. Rev.* **23**, 3–13 (2007).
29. L. R. Thurlow, G. S. Joshi, A. R. Richardson, Peroxisome proliferator-activated receptor γ is essential for the resolution of *Staphylococcus aureus* skin infections. *Cell Host Microbe* **24**, 261–270.e4 (2018).
30. A. W. Maresso, O. Schneewind, Iron acquisition and transport in *Staphylococcus aureus*. *Biometals* **19**, 193–203 (2006).
31. J. E. Cassat, E. P. Skaar, Metal ion acquisition in *Staphylococcus aureus*: Overcoming nutritional immunity. *Semin. Immunopathol.* **34**, 215–235 (2012).
32. J. L. Hine, S. de Lusignan, D. Burleigh, S. Pathirannehelage, A. McGovern, P. Gatenby, S. Jones, D. Jiang, J. Williams, A. J. Elliot, G. E. Smith, J. Brownrigg, R. Hinchliffe, N. Munro, Association between glycaemic control and common infections in people with Type 2 diabetes: A cohort study. *Diabet. Med.* **34**, 551–557 (2017).
33. D. Schuster, J. Rickmeyer, M. Gajdiss, T. Thye, S. Lorenzen, M. Reif, M. Josten, C. Szekat, L. D. R. Melo, R. M. Schmithausen, F. Liégeois, H.-G. Sahl, J.-P. J. Gonzalez, M. Nagel, G. Bierbaum, Differentiation of Staphylococcus argenteus (formerly: *Staphylococcus aureus* clonal complex 75) by mass spectrometry from *S. aureus* using the first strain isolated from a wild African great ape. *Int. J. Med. Microbiol.* **307**, 57–63 (2017).
34. A. D. Yeap, K. Woods, D. A. B. Dance, B. Pichon, S. Rattanavong, V. Davong, R. Phetsouvanh, P. N. Newton, N. Shetty, A. M. Kearns, Molecular epidemiology of *Staphylococcus aureus* skin and soft tissue infections in the Lao People's Democratic Republic. *Am. J. Trop. Med. Hyg.* **97**, 423–428 (2017).
35. S. R. Somarajan, J. H. Roh, K. V. Singh, G. M. Weinstock, B. E. Murray, CcpA is important for growth and virulence of *Enterococcus faecium*. *Infect. Immun.* **82**, 3580–3587 (2014).
36. L. A. Vega, H. Malke, K. S. McIver, Virulence-related transcriptional regulators of *Streptococcus pyogenes*, in *Streptococcus Pyogenes: Basic Biology to Clinical Manifestations*, J. J. Ferretti, D. L. Stevens, V. A. Fischetti, Eds. (University of Oklahoma Health Sciences Center, Oklahoma City, 2016).
37. N. S. Kumar, E. M. Dullaghan, B. B. Finlay, H. Gong, N. E. Reiner, J. Jon Paul Selvam, L. M. Thorson, S. Campbell, N. Vitko, A. R. Richardson, R. Zoraghi, R. N. Young, Discovery and optimization of a new class of pyruvate kinase inhibitors as potential therapeutics for the treatment of methicillin-resistant *Staphylococcus aureus* infections. *Bioorg. Med. Chem.* **22**, 1708–1725 (2014).
38. J. R. Fuller, N. P. Vitko, E. F. Perkowski, E. Scott, D. Khatri, J. S. Spontak, L. R. Thurlow, A. R. Richardson, Identification of a lactate-quinone oxidoreductase in Staphylococcus aureus that is essential for virulence. *Front. Cell. Inf. Microbiol.* **1**, 19 (2011).
39. L. R. Thurlow, G. S. Joshi, J. R. Clark, J. S. Spontak, C. J. Neely, R. Maile, A. R. Richardson, Functional modularity of the arginine catabolic mobile element contributes to the success of USA300 methicillin-resistant Staphylococcus aureus. *Cell Host Microbe* **13**, 100–107 (2013).
40. J. M. Yarwood, J. K. McCormick, P. M. Schlievert, Identification of a novel two-component regulatory system that acts in global regulation of virulence factors of *Staphylococcus aureus*. *J. Bacteriol.* **183**, 1113–1123 (2001).
41. L. R. Thurlow, M. L. Hanke, T. Fritz, A. Angle, A. Aldrich, S. H. Williams, I. L. Engebretsen, K. W. Bayles, A. R. Horswill, T. Kielian, *Staphylococcus aureus* biofilms prevent macrophage phagocytosis and attenuate inflammation in vivo. *J. Immunol.* **186**, 6585–6596 (2011).
42. M. R. Grosser, A. Weiss, L. N. Shaw, A. R. Richardson, Regulatory requirements for *Staphylococcus aureus* nitric oxide resistance. *J. Bacteriol.* **198**, 2043–2055 (2016).
43. N. P. Vitko, N. A. Spahich, A. R. Richardson, Glycolytic dependency of high-level nitric oxide resistance and virulence in *Staphylococcus aureus*. *MBio* **6**, e00045-15 (2015).
44. M. E. Wörmann, N. T. Reichmann, C. L. Malone, A. R. Horswill, A. Grundling, Proteolytic cleavage inactivates the *Staphylococcus aureus* lipoteichoic acid synthase. *J. Bacteriol.* **193**, 5279–5291 (2011).

Acknowledgments: We thank L. Makowski for providing GLUT-1 LysM/Cre mice. We also thank B. Wang for discussions leading to the linking of Agr activity with the ATP levels and the overall energy state of the cell. **Funding:** We acknowledge funding sources for this work, namely, R01AI093613 and R21AI111707 to A.R.R. **Author contributions:** L.R.T. and A.R.R. conceived and designed the experiments. L.R.T., A.C.S., and K.E.H. conducted the experiments. L.R.T. and A.R.R. wrote the manuscript. **Competing interests:** The authors declare that they have no competing interests. **Data and materials availability:** All data needed to evaluate the conclusions in the paper are present in the paper and/or the Supplementary Materials. Additional data related to this paper may be requested from the authors.

Submitted 30 April 2020
Accepted 29 September 2020
Published 13 November 2020
10.1126/sciadv.abc5569

Citation: L. R. Thurlow, A. C. Stephens, K. E. Hurley, A. R. Richardson, Lack of nutritional immunity in diabetic skin infections promotes *Staphylococcus aureus* virulence. *Sci. Adv.* **6**, eabc5569 (2020).

Science Advances

Lack of nutritional immunity in diabetic skin infections promotes *Staphylococcus aureus* virulence

Lance R. Thurlow, Amelia C. Stephens, Kelly E. Hurley and Anthony R. Richardson

Sci Adv **6** (46), eabc5569.
DOI: 10.1126/sciadv.abc5569